Article

Discovery Medicine 2024; 36(184): 936–945
https://doi.org/10.24976/Discov.Med.202436184.87

IL-10-Mediated Regulation of Microglial Inflammation in Brain Meningitis: Novel Insights and Therapeutic Potential

Xiaopeng Li[1,†], Li Gao[1,†], Chaoliang Li[2], Biao Wang[2], Yuanmei Che[2,*]

[1]Department of Infection, First Affiliated Hospital of Nanchang University, 330000 Nanchang, Jiangxi, China
[2]Department of Infection, Jiangxi Provincial People's Hospital, 330000 Nanchang, Jiangxi, China
*Correspondence: cymyhl1105@sina.com (Yuanmei Che)
[†]These authors contributed equally.
Published: 20 May 2024

Background: Inflammation is a key pathological process in bacterial meningitis, and the transforming growth factor-beta-activated kinase 1 (TAK1)/nuclear factor-kappa B (NF-κB) pathway is implicated in the activation of microglia and the production of inflammatory factors. Interleukin (IL)-10 is an anti-inflammatory cytokine acting in an autocrine fashion in macrophages to limit inflammatory responses by decreasing the production of pro-inflammatory cytokines. This paper investigates how IL-10 can inhibit microglia activation and reduce the inflammatory response of nervous system diseases.

Methods: This study used a pneumococcal-induced in Pneumococcal meningitis (PM) C57BL/6 mice and BV-2 cells model of microglial activation, assessing the effects of IL-10 on the TAK1/NF-κB pathway. The impact of IL-10 on microglial autophagy was investigated through western blot and immunofluorescence. The effects of IL-10 were evaluated by examining cellular activation markers and the activity of molecular signaling pathways (such as phosphorylation levels of TAK1 and NF-κB).

Results: Pneumococcus induced the activation of microglia and reduced IL-10. IL-10 inhibited the TAK1/NF-κB pathway, reducing the pneumococcal-induced inflammatory response in microglia. IL-10 ameliorated pneumococcal infection-induced microglial injury by inhibiting autophagy. Animal experiment results also showed that IL-10 inhibited inflammation and autophagy during Pneumococcal meningitis in mice.

Conclusion: Our study demonstrates that IL-10 reduces the inflammatory response of microglia by inhibiting the TAK1/NF-κB pathway. Additionally, IL-10 ameliorates pneumococcal infection-induced microglial injury by inhibiting the process of autophagy. These results provide a new theoretical basis and offer new insights for developing strategies to treat bacterial meningitis.

Keywords: bacterial meningitis; IL-10; TAK1/NF-κB pathway; microglia; inflammatory response

Introduction

Pneumococcal meningitis (PM) is a severe infectious disease primarily caused by *Streptococcus pneumoniae* (*S. pneumoniae*) [1,2]. This disease is common in infants and individuals with compromised immunity and carries a high risk of mortality and disability [3]. As vital immune cells in the central nervous system, microglia play a crucial role during pneumococcal infection [4,5]. The activation of microglia and the resulting inflammatory response are essential components of the immune system's response to infection; however, excessive inflammation and cell injury can lead to neurological damage and functional impairments [6,7].

Interleukin (IL)-10 is an important immunoregulatory factor with anti-inflammatory effects [8]. Previous studies have demonstrated that IL-10 can inhibit inflammatory responses in various cell types including CD4 and CD8 T cells, B cells, etc. [9,10]. However, the mechanisms and effects of IL-10 in PM are not fully understood [11]. The transforming growth factor-beta-activated kinase 1 (TAK1)/nuclear factor-kappa B (NF-κB) pathway is an important signaling pathway in inflammatory responses, and its activation can trigger the release of various inflammatory mediators and the occurrence of inflammation [12,13]. IL-10 may regulate inflammatory responses by inhibiting the NF-κB pathway [14–16]. However, it is unclear whether IL-10 regulates the inflammatory response of microglia in PM by inhibiting the TAK1/NF-κB pathway. Autophagy is a cellular process involved in the clearance of intracellular waste and protein degradation, and it can regulate cell metabolism and survival [17]. Recent studies have shown that autophagy also plays a vital role in inflammatory responses [18–20]. However, whether IL-10 affects the inflammatory response by regulating autophagy in microglia during PM is unclear.

Therefore, this study aims to investigate the mechanisms of IL-10 in PM, particularly its regulatory effects on

autophagy and inflammatory responses in microglia. We studied the effects of IL-10 on the activation status of microglia, the production of inflammatory factors, and autophagy through *in vitro* and *in vivo* experiments. We further explored whether IL-10 regulates the inflammatory response of microglia by inhibiting the TAK1/NF-κB pathway and investigated the effects of IL-10 on microglial autophagy. These experiments aim to reveal the mechanisms of IL-10 in PM and provide new insights and strategies for treating this disease.

Methods

Cell Culture

BV-2 cells (CBP60922, ATCC, Manassas, VA, USA) were cultured in high-glucose Dubellco's Modified Essential Medium (DMEM, CM15019, MACGENE, Beijing, China) medium supplemented with 10% fetal bovine serum (FBS; FCS500, EXcellBio, Suzhou, China). The cells were maintained in a humidified incubator at 37 °C with 5% CO_2. Cells were passaged using 0.25% trypsin when they reached over 80% confluency. Subsequent treatments were performed when the cells entered the logarithmic growth phase. *S. pneumoniae* (5×10^5 CFU/well) was co-incubated with BV-2 cells (5×10^5 cells per well) (as to *S. pneumoniae* group) in DMEM supplemented with 10% fetal bovine serum for 24 hours (37 °C, 5% CO_2) with gentle shaking (150 r.p.m.). Then, 20 ng/mL IL-10 (HY-P70517, MedChemExpress, Monmouth Junction, NJ, USA) was administered as reparative BV-2 cells (as to the *S. pneumoniae* + IL-10 group) in 24 hours and used in subsequent experiments. BV-2 cells without any treatment served as a negative control (control). BV-2 microglial cells were incubated for 2 hours with Brefeldin A (5 µg/mL, 20350-15-6, Saint Louis, MO, USA) and then infected with *S. pneumoniae* at a multiplicity of infection (MOI) of 50 for 8 hours. All cell lines were mycoplasma-free when periodically tested using the Mycoalert assay (LT07-318, Lonza, Rockland, ME, USA), and all cell lines have been authenticated through Short Tandem Repeats (STR) analysis.

Enzyme-Linked Immunosorbent Assay (ELISA) Detection

The ELISA assay was performed according to the instructions ELISA kit (Wuhan Saipei Biotechnology Co., Ltd., Wuhan, China) of tumor necrosis factor-alpha (TNF-α; SP10205), IL-6 (SP10234), IL-4 (SP10236), and lactate dehydrogenase (LDH; SP10441) and centrifuged to remove debris. The prepared avidin-biotin-peroxidase complex (ABC) and 3,3′,5,5′-tetramethylbenzidine (TMB) chromogenic solutions were equilibrated at 37 °C for 30 min. Then, 100 µL of the sample was added and incubated at 37 °C for 1.5 hours. The liquid in the ELISA plate was removed, and 100 µL of biotinylated antibody was added to each well. The ABC working solution (100 µL per well) was added sequentially (except for the TMB blank wells). Then, 90 µL of the equilibrated TMB chromogenic solution was added to each well at 37 °C. The plate was incubated at 37 °C for 15–20 min for color development, and 100 µL of TMB stop solution was added. The OD values were measured at 450 nm using a microplate reader (VLBL0TD2, BioTek, Winooski, VT, USA).

Table 1. Sequences of primers for fluorescence quantification.

Name	Primer sequences (5′-3′)
IL-10	F: TGGGTTGCCAAGCCTTATCG R: GGTCTTCAGCTTCTCACCCA
Beclin1	F: GAGGGATGGAAGGGTCTA R: GCCTGGGCTGTGGTAAGT
ATG5	F: TTTGCATCACCTCTGCTTTC R: TAGGCCAAAGGTTTCAGCTT
GAPDH	F: GGAGCGAGATCCCTCCAAAAT R: GGCTGTTGTCATACTTCTCATGG

IL-10, interleukin-10; *ATG5*, autophagy-related gene 5; *GAPDH*, glyceraldehyde-3-phosphate dehydrogenase; F, forward; R, reverse.

Quantitative Reverse Transcriptase Polymerase Chain Reaction (qRT-PCR)

The assay was performed by the TAKARA RNA extraction kit (9767, Baori Doctor Physical Technology Co., Ltd., Beijing, China). The reaction system and program were carried out according to the manufacturer's instructions. The reaction system (25 µL) consisted of 5 µL of RNA template, 0.5 µL of Taq enzyme, 0.5 µL of reverse transcriptase, and 14 µL of PCR reaction solution. The reaction program included pre-denaturation at 95 °C for 5 min, denaturation at 95 °C for 15 seconds, annealing at 58 °C for 15 seconds, extension at 72 °C for 40 seconds, and a total of 40 cycles. The detection data were recorded and analyzed using specific software. The $2^{-\Delta\Delta Ct}$ equation was used to examine each gene's expression. The primer sequences are shown in Table 1.

Western Blot

Cells were first washed with pre-cooled phosphate-buffered saline (PBS) at 4 °C, followed by lysis using 100 µL of protein lysis buffer. After homogenization and centrifugation, the supernatant containing the proteins was collected. Subsequently, 30 µg of protein samples were separated by sodium dodecyl sulfate-polyacrylamide gel electrophoresis (SDS-PAGE) and transferred onto a polyvinylidene fluoride (PVDF) membrane. The membrane was then blocked with 5% non-fat milk at room temperature for 1 hour. Primary antibodies including phosphate (p)-TAK1 (1:2000, ab109404, Abcam, Cambridge, United Kingdom), TAK1 (1:2000, ab109526, Abcam, Cambridge, United

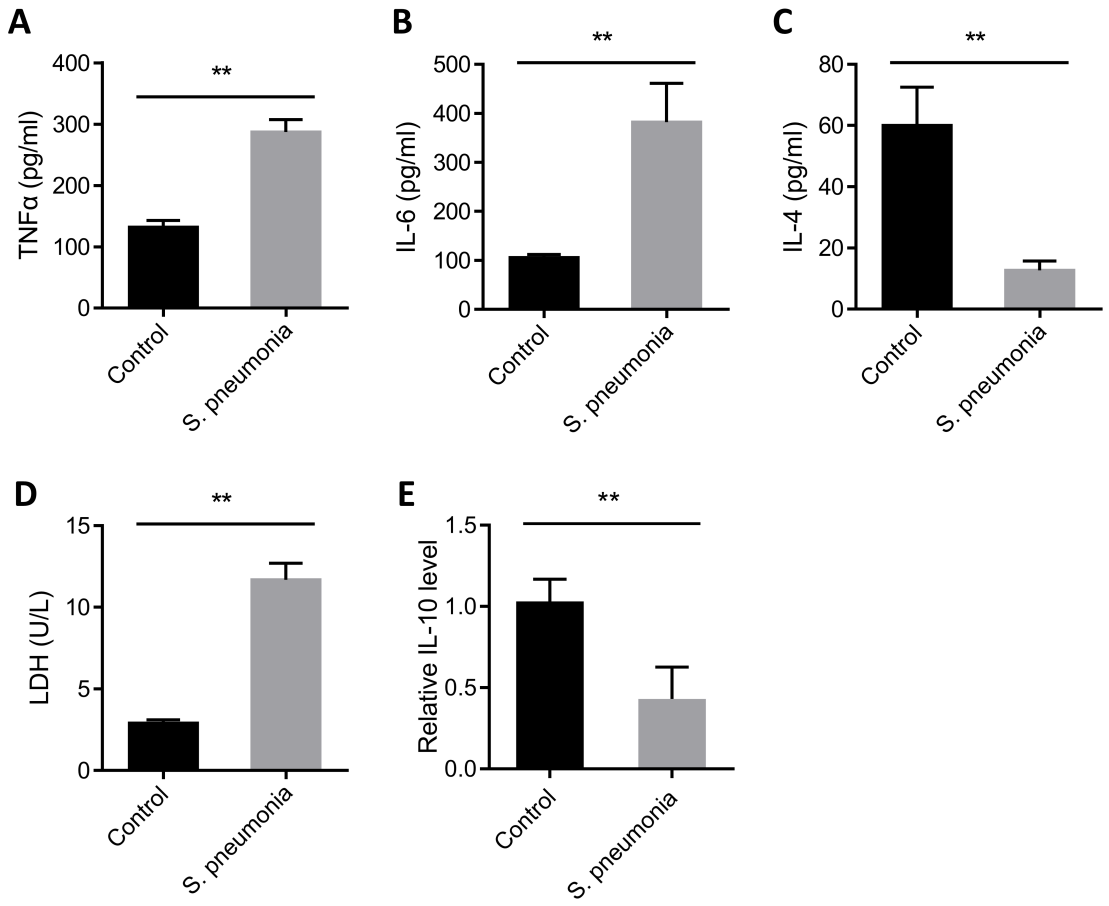

Fig. 1. *S. pneumoniae* induces microglial activation and decreases Interleukin (IL)-10 levels. BV-2 microglial cells were either uninfected or infected with *S. pneumoniae* at a multiplicity of infection (MOI) of 50 for 24 hours. (A–C) Levels of tumor necrosis factor-alpha (TNF-α) (A), IL-6 (B), and IL-4 (C) were measured. (D) Lactate dehydrogenase (LDH) level. (E) Expression of *IL-10* in cell lysates was analyzed by quantitative reverse transcriptase polymerase chain reaction (qRT-PCR). N = 5. $^{**}p < 0.01$. *S. pneumoniae*, *Streptococcus pneumoniae*.

Kingdom), p-p65 (1:2000, ab31624, Abcam, Cambridge, United Kingdom), p65 (1:1000, ab32536, Abcam, Cambridge, United Kingdom), light chain 3 (LC3) I/II (1:1000, ABC929, Sigma-Aldrich, Burlington, MA, USA), Beclin1 (1:1000, ab302669, Abcam, Cambridge, United Kingdom), and autophagy-related gene 5 (ATG5) (1:1000, ab108327, Abcam, Cambridge, United Kingdom) were incubated with the membrane. After three washes with TBST buffer for 15 minutes each, the membrane was incubated with Rabbit Anti-Mouse IgG H&L secondary antibody (1:10000, ab6728, Abcam, Cambridge, United Kingdom). Following another three washes with TBST buffer for 15 min each, visualizing with SuperSignal Chemiluminescent horseradish peroxidase (HRP) Substrate and photographing with software Image Lab version in ChemiDoc MP Imaging System (Version No. 6.0.34; Bio-Rad, Hercules, CA, US). The Pro Plus software (Image-Pro Plus 5.1, Media Cybernetics, Inc., Rockville, MD, USA) was used for protein quantification.

Immunofluorescence Staining

Fixed cells were treated with 4% paraformaldehyde. Permeabilization was achieved by incubating the cells with 0.1% Triton X-100, allowing the antibodies to penetrate the cell membrane. To block non-specific binding, the cells were treated with a working solution of goat serum for 20 min, followed by the removal of the serum. The cells were incubated overnight at 4 °C with a diluted primary antibody targeting LC3A/B (1:250, #4180, Cell Signaling Technology, Denver, MA, USA). Incubated with a diluted fluorescent secondary antibody, specifically goat anti-rabbit IgG H&L conjugated with Alexa Fluor 488 (1:500, Biotium, Fremont, CA, USA). A 4′,6-diamidino-2-phenylindole (DAPI) working solution containing Irving Blue (0.5%, D9542, Sigma, Saint Louis, MO, USA) was added to visualize the cell nuclei. The stained cells were then observed and photographed using a confocal microscope (OLYMPUS DP80, Olympus Co., Tokyo, Japan).

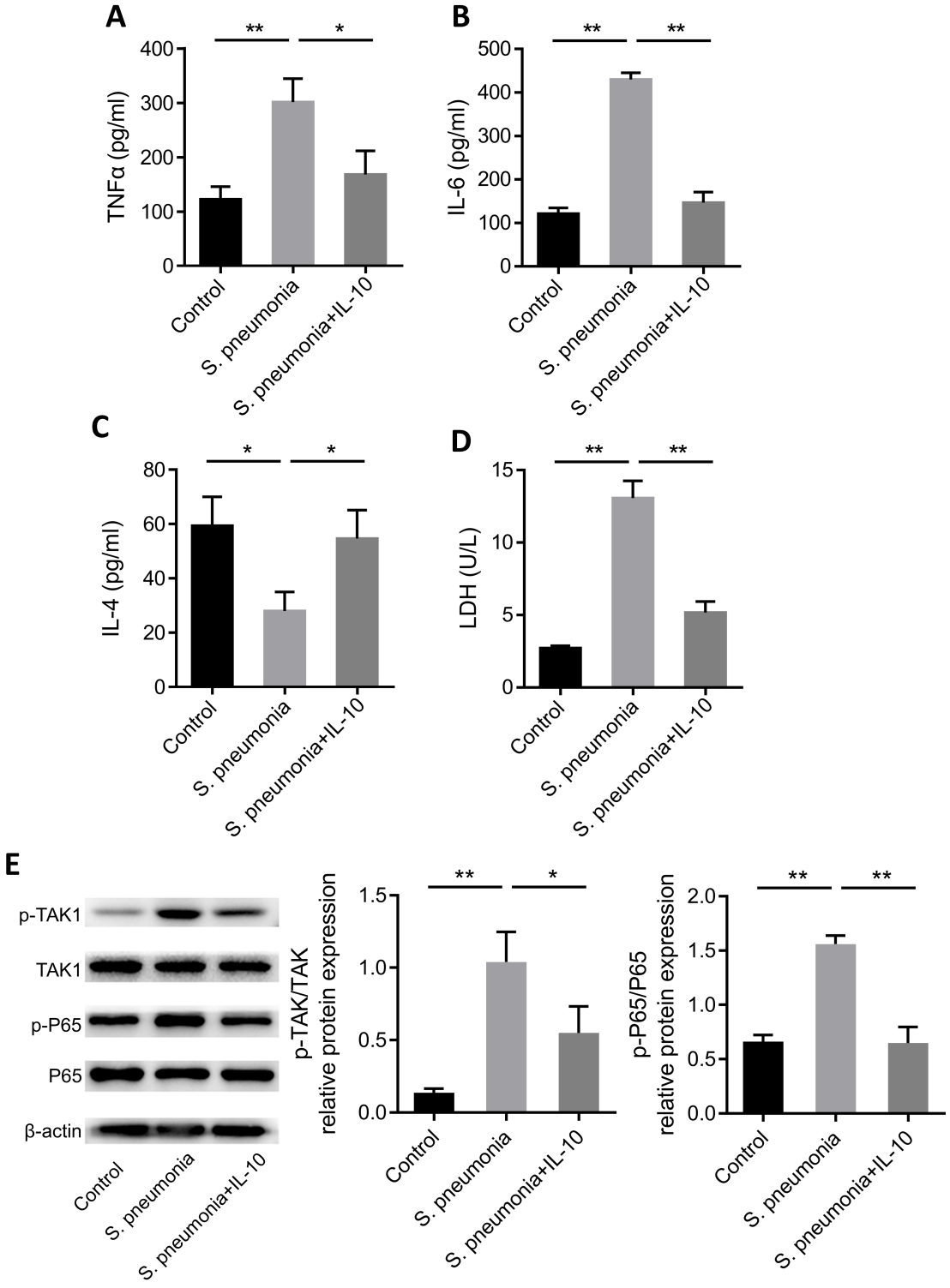

Fig. 2. IL-10 inhibits the transforming growth factor-beta-activated kinase 1 (TAK1)/nuclear factor-kappa B (NF-κB) pathway and reduces *S. pneumoniae*-induced microglial inflammation. (A–C) Levels of TNF-α (A), IL-6 (B), and IL-4 (C). (D) LDH level. (E) Changes in TAK1/NF-κB pathway-related proteins in cell lysates and representative images. N = 5. *$p < 0.05$, **$p < 0.01$.

Intracerebroventricular Injection of S. pneumoniae-Induced Meningitis

Experimental animals, eighteen C57BL/6 mice (190–230 g) aged 6–8 weeks, were purchased from Beijing Huafukang Biotechnology Co., Ltd. The mice were divided into the following 3 groups (6 animals per group): (i) phosphate-buffered saline control (control group); (ii) *S. pneumoniae* model (SP group); (iii) IL-10 (*S. pneumoniae* + IL-10 at 0.1 mg/kg)-treated group. The 18 mice were anesthetized by intraperitoneal injection of sodium pentobarbital (50 mg/kg),

and their heads were fixed on the brain stereotaxic apparatus. The standard strain of *S. pneumoniae* serotype III (ATCC 6303) was stored at –80 °C and inoculated on blood agar plates. The bacteria were cultured at 37 °C with 5% CO_2 for 16 hours. After scraping the colonies from the plates, the bacteria were resuspended in physiological saline and adjusted to an absorbance of 0.5 at 620 nm (approximately 1×10^9 CFU/mL). The mice were either actively immunized and challenged with *S. pneumoniae* after two weeks or passively immunized and immediately challenged to establish the meningitis model. The intracerebroventricular injection method [21,22] was used, with the injection site located approximately 0.5 mm posterior to the bregma and 1.0 mm right of the midline at a vertical depth of 3.0 mm. A volume of 15 µL of the standard strain of *S. pneumoniae* serotype III was injected at a dose of 5×10^6 CFU/mouse. The animals were monitored daily by measuring weight and evaluating neurological deficit scores. After the experiment, the mice were euthanized by inhaling carbon dioxide. This study has been approved by the Medical Ethics Committee of Jiangxi Provincial People's Hospital (approval number: KT018).

Spontaneous Locomotor Activity Test in Mice

The spontaneous locomotor activity test in mice was conducted using a running wheel, an infrared detection device, and a data analysis system. The running wheel was placed in an environment control box, which maintained a temperature of (22 ± 2) °C and provided isolation from external noise and light. The box also facilitated automatic light-dark cycles based on the experimental requirements. The infrared detection device was utilized to capture the mice's locomotor activity, and the data analysis system was employed to collect and analyze the recorded data. The clinical disease status was examined by spontaneous motor activity [21]. The following scores were used to assess the spontaneous motor activity of mice as described previously (7): 5 points, normal motor activity and turned upright in <5 sec when put on its back; 4 points, decreased spontaneous activity, but turned upright in <5 sec; 3 points, turned upright in >5 sec; 2 points, did not turn upright; and 1 point, did not move or coma.

Brain Tissue Water Content Measurement

The wet-dry method was employed to determine the brain tissue's water content. A dry weighing cup was used to hold the left brain tissue, which was then weighed using an electronic analytical balance to obtain the initial wet weight. Subsequently, the brain tissue was dried in a 100 °C oven until a constant weight was achieved (with a difference of ≤0.2 mg between two measurements), providing the dry weight of the tissue. Formula = (wet weight – dry weight)/wet weight × 100%.

Statistical Analysis

The statistical analysis was conducted utilizing SPSS (version 22, Armonk, NY, USA) and GraphPad Prism software (version 8.0.2, New York City, NY, USA). The mean ± SD values were used to present the results. To compare control and *S. pneumoniae* groups, *t*-tests were employed. A one-way ANOVA was utilized for control, *S. pneumoniae*, and *S. pneumoniae* + IL-10 group comparisons, followed by the Student-Newman-Keuls post hoc test for pairwise comparisons. Statistical significance was defined as a p value of <0.05.

Results

S. pneumoniae Induces Microglial Activation and Reduces IL-10 Levels

TNF-α and IL-6 in the *S. pneumoniae* infection group were higher ($p < 0.01$), indicating that *S. pneumoniae* infection can stimulate microglia to produce TNF-α and IL-6, thereby triggering an inflammatory response (Fig. 1A,B). IL-4 in the *S. pneumoniae* infection group was lower ($p < 0.01$), indicating that *S. pneumoniae* infection can reduce the production of IL-4 by microglia, thereby weakening the anti-inflammatory response (Fig. 1C). ELISA results showed that the release of LDH in the *S. pneumoniae* infection group was higher ($p < 0.01$), indicating that *S. pneumoniae* infection can cause damage and death of microglia (Fig. 1D). *IL-10* in the control group was higher ($p < 0.01$) than that in the *S. pneumoniae* infection group, indicating that *S. pneumoniae* infection can reduce the production of *IL-10* by microglia (Fig. 1E).

IL-10 Inhibits the TAK1/NF-κB Pathway to Reduce the Inflammatory Response of S. pneumoniae-Induced Microglia

TNF-α and IL-6 were highest ($p < 0.01$) in the *S. pneumoniae* infection group, while they were reduced ($p < 0.05$) in the *S. pneumoniae* + IL-10 group (Fig. 2A,B). This suggests that *S. pneumoniae* infection stimulated microglia to produce TNF-α and IL-6, and the addition of IL-10 partially inhibited TNF-α and IL-6. IL-4 was lowest ($p < 0.05$) in the *S. pneumoniae* infection group, while it increased ($p < 0.05$) in the *S. pneumoniae* + IL-10 group. The addition of IL-10 partially restored the production of IL-4 (Fig. 2C). The *S. pneumoniae* infection group released the most LDH from BV-2 microglia, while the release of LDH was reduced ($p < 0.01$) in the *S. pneumoniae* + IL-10 group (Fig. 2D). These results indicate *S. pneumoniae* infection causes damage and death in microglia. The addition of IL-10 partially reduced cell damage. Western blot analysis of cell lysates was performed to detect changes in TAK1/NF-κB pathway-related proteins. 24 h after *S. pneumoniae* infection, p-TAK1, and p-p65 were upregulated ($p < 0.01$) compared to the control group. IL-10 inhibited the activation of the TAK1/NF-κB pathway (Fig. 2E).

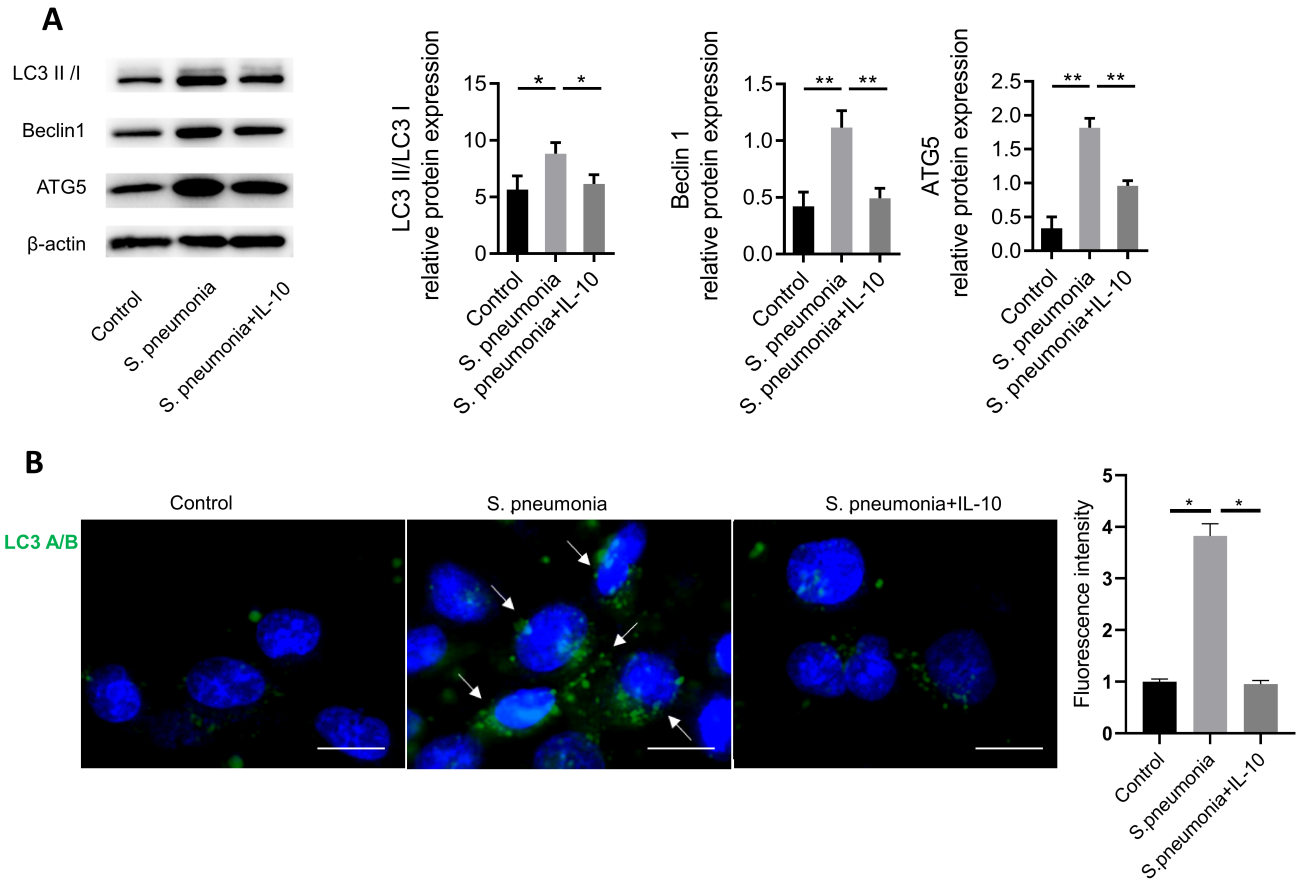

Fig. 3. The autophagy induced by *S. pneumoniae* infection was inhibited by IL-10. (A) Light chain 3 (LC3), Beclin1, and autophagy-related gene 5 (ATG5) expression. (B) Representative images and Immunofluorescence (IF) analysis of LC3. White arrows indicate the green staining of LC3 puncta. Scale bar = 10 µm. N = 5. *$p < 0.05$, **$p < 0.01$.

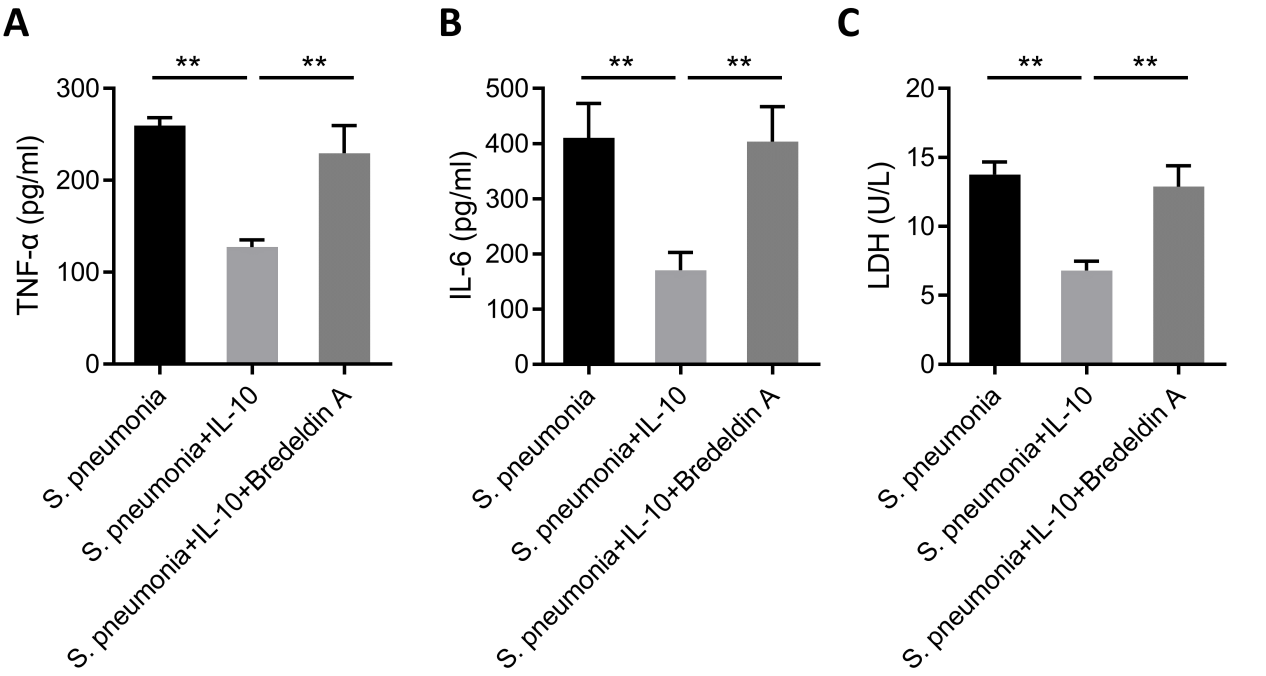

Fig. 4. IL-10 attenuated Bredeldin A-induced autophagy. BV-2 microglial cells were incubated for 2 hours with Brefeldin A and then infected with *S. pneumoniae* at an MOI of 50 for 8 hours. (A,B) Levels of TNF-α (A) and IL-6 (B). (C) LDH levels. N = 5. **$p < 0.01$.

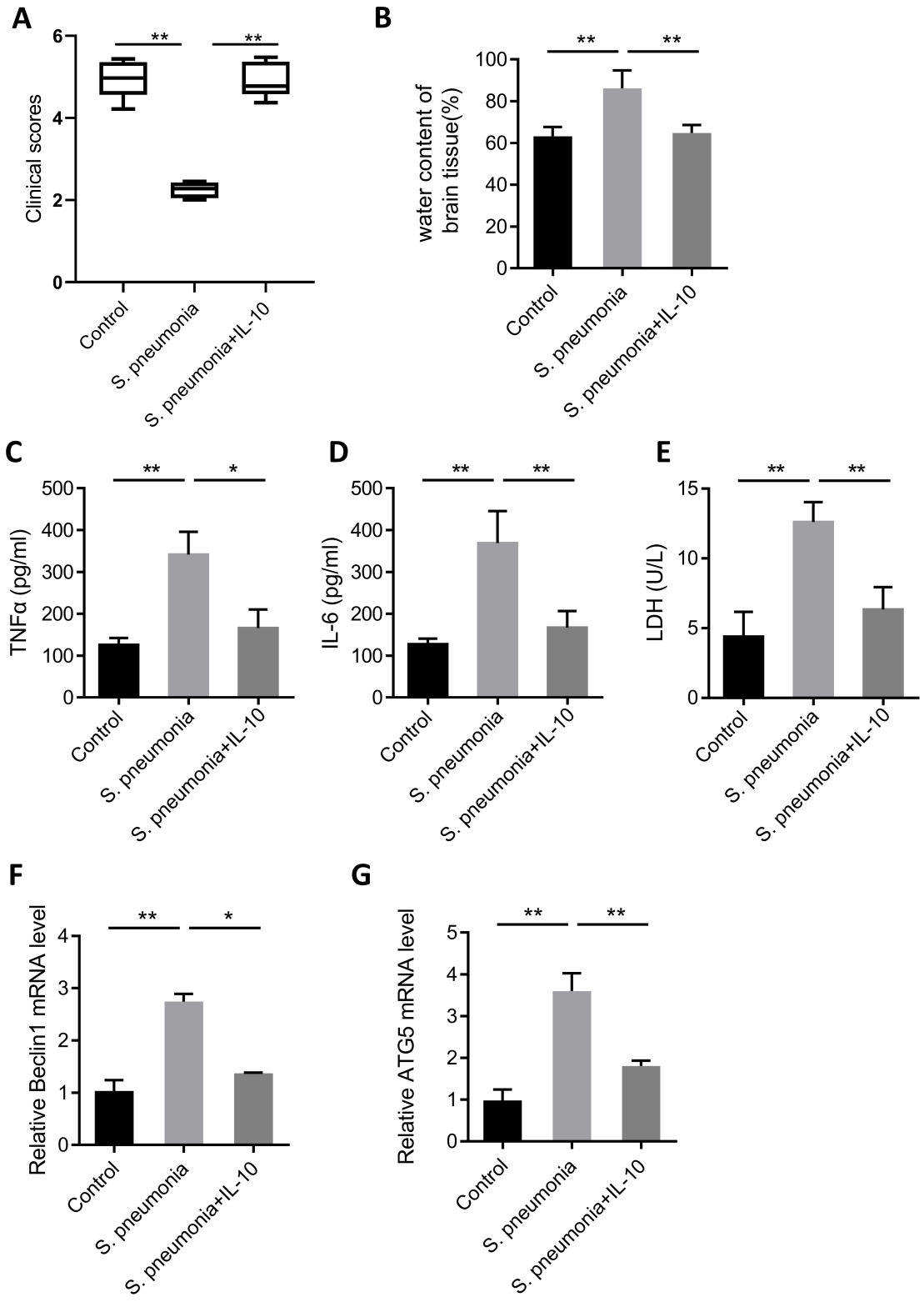

Fig. 5. IL-10 inhibits inflammation and autophagy during *S. pneumoniae*-induced meningitis in mice. Meningitis was induced by intraventricular injection of *S. pneumoniae* in C57BL/6 mice and intraventricularly injected with IL-10. (A) The clinical disease status. (B) The water content of the brain was evaluated 24 hours after the *S. pneumoniae* infection. (C,D) Levels of TNF-α (C) and IL-6 (D) in the brain tissue homogenate were measured by enzyme-linked immunosorbent assay (ELISA). (E) LDH level. (F,G) Expression of Beclin1 (F) and *ATG5* (G). N = 5. *$p < 0.05$, **$p < 0.01$.

The Autophagy Induced by S. pneumoniae Infection was Inhibited by IL-10

LC3, Beclin1, and ATG5 were analyzed by western blot. In the *S. pneumoniae* infection group, LC3-II/LC3-I were higher ($p < 0.05$), as well as Beclin1 and ATG5. However, in the *S. pneumoniae* + IL-10 group, LC3-II/LC3-I were decreased ($p < 0.01$), along with Beclin1 and ATG5 (Fig. 3A). These results indicate that IL-10 can inhibit the autophagy process in microglia induced by *S. pneumoniae* infection. In Fig. 3B, BV-2 cells were stained with anti-LC3 antibodies to observe the formation of anti-LC3 puncta. More anti-LC3 puncta (green) were formed in BV-2 cells after 24 hours of *S. pneumoniae* infection. However, in the *S. pneumoniae* + IL-10 group, the formation of anti-LC3 puncta was reduced.

IL-10 Attenuated Bredeldin A-Induced Autophagy

Bredeldin A, an autophagy inducer, was used to activate the autophagy process in BV-2 microglial cells to observe the effects of IL-10-mediated inhibition of autophagy on *S. pneumoniae* infection. In the *S. pneumoniae* group, TNF-α, IL-6, and LDH were higher ($p < 0.01$). However, in the *S. pneumoniae* + IL-10 group, after 24 hours, TNF-α, IL-6, and LDH were decreased ($p < 0.01$). In the *S. pneumoniae* + IL-10 + Bredeldin A group, TNF-α, IL-6, and LDH were further increased (Fig. 4A–C). These results indicate that IL-10-mediated inhibition of autophagy can reduce the release of inflammatory mediators and microglial damage caused by *S. pneumoniae* infection.

IL-10 Suppresses Inflammation and Autophagy during S. pneumoniae Meningitis in Mice

Spontaneous locomotor activity is one of the indicators used to assess mouse health condition. After 24 hours of *S. pneumoniae* infection, the spontaneous locomotor activity of mice decreased ($p < 0.01$). However, the *S. pneumoniae* + IL-10 group was partially restored (Fig. 5A). After 24 h of *S. pneumoniae* infection, the water content of brain tissue was increased ($p < 0.01$). However, in the *S. pneumoniae* + IL-10 group, the water content of brain tissue was reduced ($p < 0.01$) (Fig. 5B). In the *S. pneumoniae* 24-h group, TNF-α, IL-6, and LDH increased ($p < 0.01$). However, in the *S. pneumoniae* + IL-10 group, TNF-α, IL-6, and LDH were reduced ($p < 0.01$) (Fig. 5C–E). Detect Beclin1 and *ATG5* in brain tissue homogenates from different treatment groups. In the *S. pneumoniae* 24-h group, Beclin1, and *ATG5* were increased ($p < 0.01$). However, in the *S. pneumoniae* + IL-10 group, Beclin1 and *ATG5* were reduced ($p < 0.01$) (Fig. 5F,G). These results suggest that IL-10 can suppress autophagy-related proteins in mouse brain tissue during *S. pneumoniae* infection.

Discussion

Bacterial meningitis is a severe neurological infection, and its pathogenesis is closely related to inflammatory responses and microglial activation [23–25]. In this study, we found that IL-10 reduces the inflammatory response of microglia by inhibiting the TAK1/NF-κB pathway. This finding is of importance for a deeper understanding of the immunoregulatory role of IL-10 and its potential in treating inflammatory diseases.

IL-10 is an immunoregulatory factor [8]. IL-10 can inhibit various immune cells' activation and inflammatory response, including microglia [11,26–28]. Microglia play a crucial role in neurodegenerative diseases [29,30]. Therefore, exploring the mechanisms of IL-10 in microglia is of great significance for understanding the role of immune regulation and inflammation in neurological diseases [31]. Our results showed that IL-10 treatment inhibits the activation of the TAK1/NF-κB pathway in microglia. TAK1 is a key signaling molecule that regulates various cellular signaling pathways, including the NF-κB pathway [32]. Our findings suggest that IL-10 can inhibit the activation of NF-κB by suppressing TAK1 activation, thereby reducing the inflammatory response of microglia. This discovery reveals the crucial role of IL-10 in regulating the inflammatory response of microglia.

Degradation of the endoplasmic reticulum (ER), termed ER-phagy (reticulophagy), has been found to play a vital role in human sensory neuropathy. Endoplasmic reticulum stress inducer brefeldin A (BFA) blocks protein transport between the ER and Golgi apparatus [33]. We also found that IL-10 treatment promotes autophagy in microglia brefeldin A-induced. Autophagy is a cellular garbage clearance mechanism that maintains cellular homeostasis by degrading and recycling damaged proteins and organelles [18]. Autophagy also plays an important role in immune regulation and inflammation [34]. Our results showed that IL-10 treatment reduces the accumulation of the autophagy-related protein LC3-II in microglia, suggesting that IL-10 can regulate the inflammatory response of microglia by inhibiting autophagy. We also found that IL-10 treatment reduces the production of inflammatory factors in microglia, including LDH, IL-6, and TNF-α. This further confirms the anti-inflammatory effects of IL-10. Our results indicate that IL-10 can reduce microglia's inflammatory response and damage by inhibiting the TAK1/NF-κB pathway and suppressing autophagy. Our cell-level findings and animal experiments further validate the anti-inflammatory effects of IL-10, indicating its potential in the treatment of inflammatory diseases.

Although our study provides new evidence for the potential of IL-10 in the treatment of inflammatory diseases, there are still some limitations. As an immune regulatory factor, IL-10 may have immunosuppressive side effects during treatment. Therefore, further research is needed to

investigate the safety and dosage selection of IL-10. In addition, our study did not explore other potential signaling pathways and factors involved in microglial activation and inflammatory response. Therefore, further research is needed to investigate other potential regulatory mechanisms.

Conclusion

In conclusion, our findings demonstrate that IL-10 reduces the inflammatory response in microglia by inhibiting the TAK1/NF-κB pathway. This discovery is of great importance for further understanding the immunoregulatory role of IL-10. Further research on the mechanisms of IL-10 action and its therapeutic efficacy in animal models will contribute to a better understanding of its potential in the treatment of inflammatory diseases. However, further studies are needed to investigate the safety, dosage selection, and other potential regulatory mechanisms of IL-10 to exploit its therapeutic potential fully.

Availability of Data and Materials

The original contributions presented in the study are included in the article, further inquiries can be directed to the corresponding author.

Author Contributions

The design of the study: YC, LG; drafting the research paper, acquiring the data: CL; analysis and interpretation of data: BW; conception and design, and finalizing the version: XL. All authors have been involved in revising it critically for important intellectual content. All authors have given final approval of the version to be published. All authors have participated sufficiently in the work to take public responsibility for appropriate portions of the content and agreed to be accountable for all aspects of the work in ensuring that questions related to its accuracy or integrity are appropriately investigated and resolved. related to its accuracy or integrity.

Ethics Approval and Consent to Participate

This study has been approved by the Medical Ethics Committee of Jiangxi Provincial People's Hospital (approval number: KT018).

Acknowledgment

Not applicable.

Funding

This research was funded by Jiangxi Provincial Natural Science Foundation (20202BAB206061).

Conflict of Interest

The authors declare no conflict of interest.

References

[1] Mohanty T, Fisher J, Bakochi A, Neumann A, Cardoso JFP, Karlsson CAQ, *et al*. Neutrophil extracellular traps in the central nervous system hinder bacterial clearance during pneumococcal meningitis. Nature Communications. 2019; 10: 1667.

[2] Tsang RSW. A Narrative Review of the Molecular Epidemiology and Laboratory Surveillance of Vaccine Preventable Bacterial Meningitis Agents: *Streptococcus pneumoniae*, *Neisseria meningitidis*, *Haemophilus influenzae* and *Streptococcus agalactiae*. Microorganisms. 2021; 9: 449.

[3] Zhang XX, Guo LY, Liu LL, Shen A, Feng WY, Huang WH, *et al*. The diagnostic value of metagenomic next-generation sequencing for identifying Streptococcus pneumoniae in paediatric bacterial meningitis. BMC Infectious Diseases. 2019; 19: 495.

[4] Wang G, Fu Y, Ma K, Liu J, Liu X. NOD2 regulates microglial inflammation through the TAK1-NF-κB pathway and autophagy activation in murine pneumococcal meningitis. Brain Research Bulletin. 2020; 158: 20–30.

[5] Qiao N, Zhang J, Zhang Y, Liu X. Synergistic regulation of microglia differentiation by CD93 and integrin β1 in the rat pneumococcal meningitis model. Immunology Letters. 2022; 251-252: 63–74.

[6] Su Y, Ma G, Zheng Y, Qin J, Li X, Ge Q, *et al*. Neonatal Meningitis-Causing *Escherichia coli* Induces Microglia Activation which Acts as a Double-Edged Sword in Bacterial Meningitis. International Journal of Molecular Sciences. 2023; 24: 9915.

[7] Thorsdottir S, Henriques-Normark B, Iovino F. The Role of Microglia in Bacterial Meningitis: Inflammatory Response, Experimental Models and New Neuroprotective Therapeutic Strategies. Frontiers in Microbiology. 2019; 10: 576.

[8] Dowling JK, Afzal R, Gearing LJ, Cervantes-Silva MP, Annett S, Davis GM, *et al*. Mitochondrial arginase-2 is essential for IL-10 metabolic reprogramming of inflammatory macrophages. Nature Communications. 2021; 12: 1460.

[9] Steen EH, Wang X, Balaji S, Butte MJ, Bollyky PL, Keswani SG. The Role of the Anti-Inflammatory Cytokine Interleukin-10 in Tissue Fibrosis. Advances in Wound Care. 2020; 9: 184–198.

[10] Saraiva M, Vieira P, O'Garra A. Biology and therapeutic potential of interleukin-10. The Journal of Experimental Medicine. 2020; 217: e20190418.

[11] Sun Y, Ma J, Li D, Li P, Zhou X, Li Y, *et al*. Interleukin-10 inhibits interleukin-1β production and inflammasome activation of microglia in epileptic seizures. Journal of Neuroinflammation. 2019; 16: 1–13.

[12] Duan Z, Xing J, Shi H, Wang Y, Zhao C. The matrix protein of Newcastle disease virus inhibits inflammatory response through IRAK4/TRAF6/TAK1/NF-κB signaling pathway. International Journal of Biological Macromolecules. 2022; 218: 295–309.

[13] Ma H, Meng Z, Zhou L, Feng H, Wu X, Xin Y, *et al*. Ferulic acid attenuated difenoconazole-induced immunotoxicity in carp by inhibiting TRAF/TAK1/NF-κB, Nrf2 and p53 pathways. Ecotoxicology and Environmental Safety. 2023; 262: 115339.

[14] Saleem A, Saleem M, Akhtar MF, Shahzad M, Jahan S. Polystichum braunii extracts inhibit Complete Freund's adjuvant-induced arthritis via upregulation of I-κB, IL-4, and IL-10, downregulation of COX-2, PGE2, IL-1β, IL-6, NF-κB, and TNF-α, and subsiding oxidative stress. Inflammopharmacology. 2020; 28: 1633–1648.

[15] Shi J, Shi S, Xie W, Zhao M, Li Y, Zhang J, *et al*. IL-

10 alleviates lipopolysaccharide-induced skin scarring via IL-10R/STAT3 axis regulating TLR4/NF-κB pathway in dermal fibroblasts. Journal of Cellular and Molecular Medicine. 2021; 25: 1554–1567.

[16] Yang L, Dong Y, Li Y, Wang D, Liu S, Wang D, *et al*. IL-10 derived from M2 macrophage promotes cancer stemness via JAK1/STAT1/NF-κB/Notch1 pathway in non-small cell lung cancer. International Journal of Cancer. 2019; 145: 1099–1110.

[17] Aman Y, Schmauck-Medina T, Hansen M, Morimoto RI, Simon AK, Bjedov I, *et al*. Autophagy in healthy aging and disease. Nature Aging. 2021; 1: 634–650.

[18] Deretic V. Autophagy in inflammation, infection, and immunometabolism. Immunity. 2021; 54: 437–453.

[19] Bharath LP, Agrawal M, McCambridge G, Nicholas DA, Hasturk H, Liu J, *et al*. Metformin Enhances Autophagy and Normalizes Mitochondrial Function to Alleviate Aging-Associated Inflammation. Cell Metabolism. 2020; 32: 44–55.e6.

[20] He ZH, Zou SY, Li M, Liao FL, Wu X, Sun HY, *et al*. The nuclear transcription factor FoxG1 affects the sensitivity of mimetic aging hair cells to inflammation by regulating autophagy pathways. Redox Biology. 2020; 28: 101364.

[21] Chen X, Wang Y, Wang Z, Yan R, Liu J, Meng X, *et al*. B7 homolog 3 aggravates brain injury in a murine model of *Streptococcus pneumoniae*-induced meningitis. Experimental and Therapeutic Medicine. 2015; 9: 1984–1990.

[22] Chen X, Bai Y, Cui W, Wang Z, Zhang G, Xu Y, *et al*. Effects of B7-H3 on the inflammatory response and expression of MMP-9 in mice with pneumococcal meningitis. Journal of Molecular Neuroscience. 2013; 50: 146–153.

[23] Sun H, Wan X, Fan Y, Liu P, Song Y, Zhu N, *et al*. Bacteria reduce flagellin synthesis to evade microglia-astrocyte-driven immunity in the brain. Cell Reports. 2022; 40.

[24] Lu HJ, Guo D, Wei QQ. Potential of Neuroinflammation-Modulating Strategies in Tuberculous Meningitis: Targeting Microglia. Aging and Disease. 2023. (online ahead of print)

[25] Woodburn SC, Bollinger JL, Wohleb ES. The semantics of microglia activation: neuroinflammation, homeostasis, and stress. Journal of Neuroinflammation. 2021; 18: 258.

[26] Han R, Lan X, Han Z, Ren H, Aafreen S, Wang W, *et al*. Improving outcomes in intracerebral hemorrhage through microglia/macrophage-targeted IL-10 delivery with phosphatidylserine liposomes. Biomaterials. 2023; 301: 122277.

[27] Laffer B, Bauer D, Wasmuth S, Busch M, Jalilvand TV, Thanos S, *et al*. Loss of IL-10 Promotes Differentiation of Microglia to a M1 Phenotype. Frontiers in Cellular Neuroscience. 2019; 13: 430.

[28] Shemer A, Scheyltjens I, Frumer GR, Kim JS, Grozovski J, Ayanaw S, *et al*. Interleukin-10 Prevents Pathological Microglia Hyperactivation following Peripheral Endotoxin Challenge. Immunity. 2020; 53: 1033–1049.e7.

[29] Chowen JA, Garcia-Segura LM. Microglia, neurodegeneration and loss of neuroendocrine control. Progress in Neurobiology. 2020; 184: 101720.

[30] Kwon HS, Koh SH. Neuroinflammation in neurodegenerative disorders: the roles of microglia and astrocytes. Translational Neurodegeneration. 2020; 9: 42.

[31] Amanollahi M, Jameie M, Heidari A, Rezaei N. The Dialogue Between Neuroinflammation and Adult Neurogenesis: Mechanisms Involved and Alterations in Neurological Diseases. Molecular Neurobiology. 2023; 60: 923–959.

[32] Zou W, Yin P, Shi Y, Jin N, Gao Q, Li J, *et al*. A Novel Biological Role of α-Mangostin via TAK1-NF-κB Pathway against Inflammatory. Inflammation. 2019; 42: 103–112.

[33] Schneider JL, Cuervo AM. Liver autophagy: much more than just taking out the trash. Nature Reviews. Gastroenterology & Hepatology. 2014; 11: 187–200.

[34] Wang Y, Zhao Z, Wei F, Luo Z, Duan Y. Combining autophagy-inducing peptides and brefeldin A delivered by perinuclear-localized mesoporous silica nanoparticles: a manipulation strategy for ER-phagy. Nanoscale. 2018; 10: 8796–8805.